PROCEEDINGS OF SCIENCE

How many vector charmonium(-like) states sit in the energy range from 4.2 to 4.35 GeV?

Leon von Detten,[a] **Vadim Baru,**[b] **Christoph Hanhart,**[a] **Qian Wang,**[c,d,e,*] **Daniel Winney**[f] **and Qiang Zhao**[e,g]

[a] *Institute for Advanced Simulation, Institut für Kernphysik and Jülich Center for Hadron Physics, Forschungszentrum Jülich, D-52425 Jülich, Germany*

[b] *Institut für Theoretische Physik II, Ruhr-Universität Bochum, D-44780 Bochum, Germany*

[c] *Key Laboratory of Atomic and Subatomic Structure and Quantum Control (MOE), Guangdong Basic Research Center of Excellence for Structure and Fundamental Interactions of Matter, Institute of Quantum Matter, South China Normal University, Guangzhou 510006, China*

[d] *Guangdong-Hong Kong Joint Laboratory of Quantum Matter, Guangdong Provincial Key Laboratory of Nuclear Science, Southern Nuclear Science Computing Center, South China Normal University, Guangzhou 510006, China*

[e] *Institute of High Energy Physics, Chinese Academy of Sciences, Beijing 100049, China*

[f] *Helmholtz-Institut für Strahlen- und Kernphysik and Bethe Center for Theoretical Physics, Universität Bonn, D-53115 Bonn, Germany*

[g] *School of Physical Sciences, University of Chinese Academy of Sciences, Beijing 100049, China*

E-mail: l.von.detten@fz-juelich.de, vadim.baru@tp2.rub.de, c.hanhart@fz-juelich.de, qianwang@m.scnu.edu.cn, daniel.winney@gmail.com, zhaoq@ihep.ac.cn

Recently, numerous vector charmonium(-like) states were reported by different electron-positron collider experiments above 4.2 GeV. However, there is no consensus on the number of these states, as the experimental analysis is based on the Breit-Wigner parametrization, which is channel-dependent. In our work, we focus on the energy region [4.2, 4.35] GeV and conduct a comprehensive analysis of eight different final states in e^+e^- annihilation. Our findings indicate that only one single charmonium-like state is sufficient to describe all the data well in the $D_1\bar{D}$ molecular picture. The extracted pole position is $\sqrt{s^{Y(4230)}_{\text{pole}}} = \left(4227\pm4-\frac{i}{2}(50^{+8}_{-2})\right)$ MeV. Beside the $D_1\bar{D}$ threshold effect which express itself as asymmetric lineshape of the $Y(4230)$, the contribution of the vector charmonium $\psi(4160)$ is necessary included perturbatively.

The XVIth Quark Confinement and the Hadron Spectrum Conference (QCHSC24)
19-24 August, 2024
Cairns Convention Centre, Cairns, Queensland, Australia

*Speaker

 ISSN 1824-8039 . Published by SISSA Medialab.

PoS(QCHSC24)123

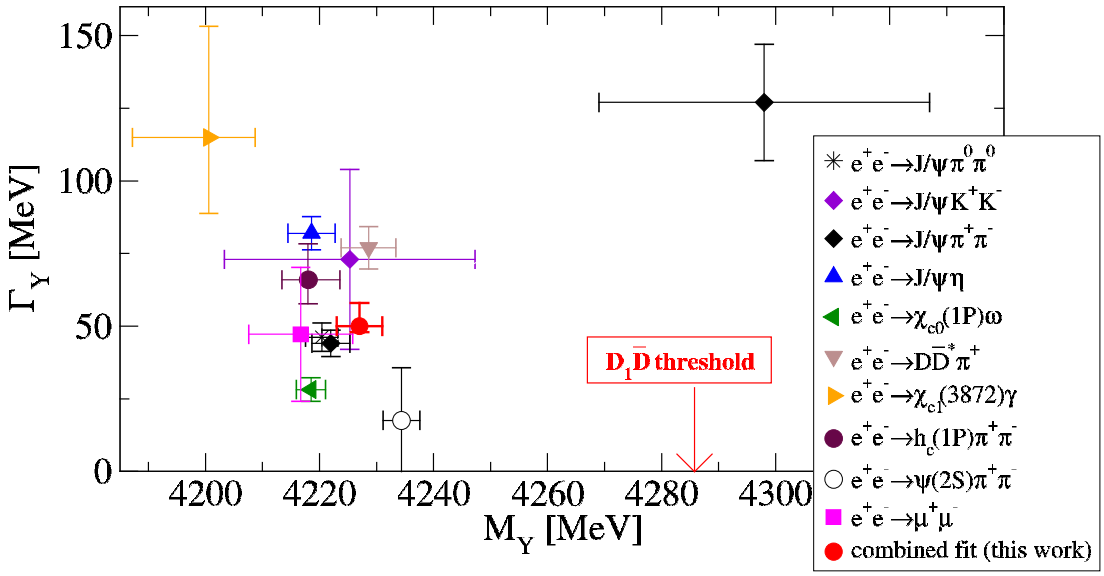

Figure 1: Mass and width of the two vector charmonium-like states in various channels. The experimental values are taken from [2, 3, 6–13]. The red dot denotes the pole location for the $Y(4230)$ as extracted in this work.

1. Introduction

Tens of exotic hadrons which are beyond the conventional quark model have been observed in experiment. Among these exotic hadrons, charmonium-like states have large statistic data in e^+e^- annihilation, for instance, BESIII collaboration has accumulated large statistic data in the energy region $[4.2, 4.35]$ GeV. In this energy region, two vector charmonium-like candidates are claimed to exist, i.e. $Y(4230)$ (also known as $\psi(4230)$) and $Y(4320)$. The latter one is introduced in the $e^+e^- \to J/\psi\pi^+\pi^-, J/\psi\pi^0\pi^0$ processes to explain the highly asymmetric line shape [1–3]. On the other hand, the $Y(4230)$ is seen in the eight additional channels shown in Fig. 1, but with largely inconsistent parameters. On the contrary, the latter $Y(4320)$ does not show up in either of them. In experiments by BaBar and Belle collaborations a state named $Y(4360)$, with a mass of about 4345 MeV, was discovered in the $\psi(2S)\pi^+\pi^-$ [4, 5] final state. However, the recent BESIII measurement of the same channel revealed that the $Y(4360)$ emerges due to a subtle interference of the $Y(4230)$ and a state at 4390 MeV with a width of 140 MeV [6], which is thus in a mass range close to the $\psi(4415)$. A signal at 4390 MeV with the consistent parameters was also observed by BESIII in the $h_c\pi\pi$ [7] and $J/\Psi\eta$ [8] final states. Since this state is outside the mass range in focus here, we do not discuss it any further.

In the interested mass region, the findings raise the following questions:

1. Why does the observed width of the $Y(4230)$ in $D^*\bar{D}\pi$ channel is twice as that in the $J/\psi\pi\pi$ channel [10]?

2. What can the different lineshapes of $Y(4230)$ in various channels tell us? Note that the $D\bar{D}^*\pi$ cross section is about one order-of-magnitude larger than those of hidden charm decays.

3. Why are the cross sections of the $Y(4230)$ in $\bar{c}c$ spin 1 (i.e. $J/\psi\pi\pi$ and $\psi'\pi\pi$ channels) and $\bar{c}c$ spin 0 (i.e. $h_c\pi\pi$ channel) are of the same order? A large HQSS violation?

4. Why is the $Y(4320)$ only seen in the $\psi(2S)\pi\pi$ channel?

5. Can we consider the apparent asymmetric lineshape in the $J/\psi\pi^+\pi^-$ channel generated by the opening of the $D_1(2420)\bar{D}$ channel?

To deepen our understanding of these vector charmonium-like states, various interpretations have been proposed. Hadroncharmonium appears as a compact $c\bar{c}$ core surrounded by some excited light quark cloud [14], which naturally explains the appearance of the $Y(4230)$ in the $J/\psi\pi\pi$ channel. In addition, its mixing with a spin singlet $c\bar{c}$ core allows for its appearance in the $h_c\pi\pi$ channel [15]. In this sense, this picture calls for another vector chamronium-like state, i.e. the $Y(4320)$ mentioned above. Moreover, this mixing scenario implies the existence of four heavy quark spin symmetry partners [16]. For example, there should be two exotic η_c states, one in between the two vector states, one significantly lighter than the $Y(4230)$. Another interpretation is hybrid scenario which is based on either phenomenological calcualtions [17–19] or heavy quark effective field theory [20]. The hybrid picture also calls for a mixing of two vector charmonium-like states with different $c\bar{c}$ spins. However, a recent study based on heavy quark effective field theory disfavors a pure hybrid interpretation of the $Y(4230)$ [21]. Another typical picture on the market is the compact tetraquark picture which is made of heavy-light diquarks and anti-diquarks. This scenario calls for four non-strange vector states with masses in the range $[4220, 4660]$ MeV [22, 23]. To obtain a negative charge parity, an angular momentum of 1 is needed between diquark and antidiquark. However, M. shifman argues that the heavy-light diquark does not exit [24] based on the heavy baryon decays in QCD chemistry. In this picture, a preferred fit should also include both $Y(4220)$ and $Y(4320)$. An alternative approach to compact tetraquarks, similar in spirit, but different in the realization, is outlined in Ref. [25]. Thus, we see that three of the non-molecular scenarios prefer the presence of both $Y(4230)$ and $Y(4320)$.

In this work, we address the above issues mentioned above in the assumption that the $Y(4230)$ is a $D_1(2420)\bar{D}$ hadronic molecule, originally proposed in Ref. [26], and refined in Ref. [27]. A similar analysis [28, 29] in the $J/\psi\pi\pi$ channel indicates that there is no need to introduce the pole of the $Y(4230)$, whose structure is generated from the $\psi(4160)$ coupling to the $D_s\bar{D}_s$ channel. However, the same scenario is unlikely to describe the other channels, especially the $D\bar{D}^*\pi$ channel. The same comment also applies to Ref. [29], where the $Y(4230)$ is generated from an interference of the neighboring charmonium states. We investigate the feasibility of a combined analysis involving eight different final states excited in e^+e^- annihilation, namely $D^0D^{*-}\pi$, $J/\psi\pi^+\pi^-$, $J/\psi K^+K^-$, $h_c\pi^+\pi^-$, $\mu^+\mu^-$, $\chi_{c0}(1P)\omega$, $J/\psi\eta$ and $X(3872)\gamma$, in the mass range from $[4.2, 5.35]$ GeV, under the assumption that the $Y(4230)$ is a $D_1\bar{D}$ molecule. [1] Moreover, the cross section of the $e^+e^- \to \mu^+\mu^-$ process is also included in our analysis.

[1] The molecular scenario for the $Y(4230)$ based on the $J/\psi\pi\pi$ and $h_c\pi\pi$ channels have already been advocated in Refs. [30, 31].

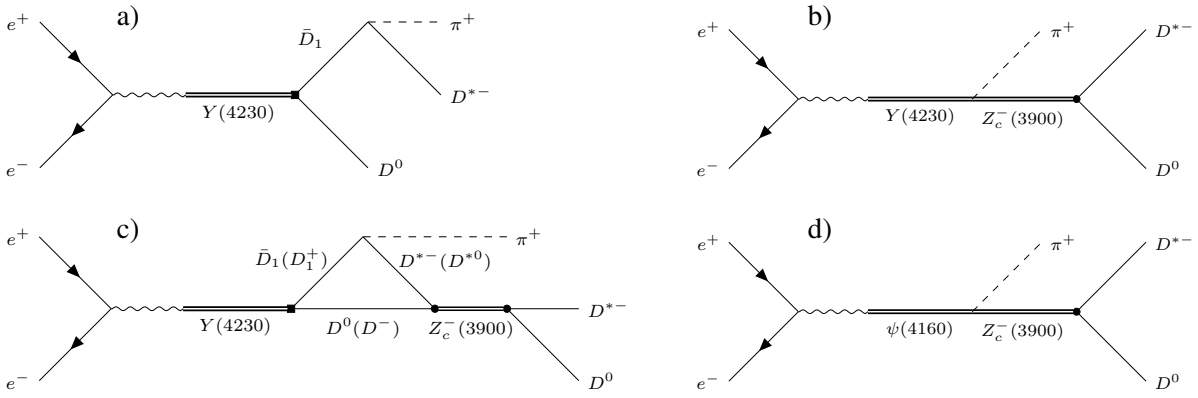

Figure 2: Diagram contributing to $e^+e^- \to \bar{D}D^*\pi$. a) tree level, b) $Y(4230)$ contact term, c) Triangle, d) $\psi(4160)$ contact term, where for the last three the final state interactions in the doubly heavy subsystem are included.

2. Fit strategy and Results

In the molecular scenario, the coupling of a dynamic generated state to the nearby foremost continuum channel is maximal [32, 33], see also [34] for a review. More specifically, in our case, the $Y(4230)$ mainly couples to the $D_1\bar{D}$ channel, and the importance of the diagrams in its decays can be analysed by the power counting scheme [35, 36]. Along this line, we present the most important diagrams for each decay channel in the following subsections. Due to the limit of the processing, we ignore the detailed formulae and the fitted parameters, which can be found in Ref. [37]. Before going to the details, we present our fit strategy at beginning:

1. The resonance parameters of the $Y(4230)$ and $Z_c(3900)$ are fitted simultaneously in the $D^0D^{*-}\pi$, $J/\psi\pi^+\pi^-$, $J/\psi K^+K^-$ and $\mu^+\mu^-$ channels, as well as these channel-dependent parameters.

2. With the above parameters fitted, the remaining parameters in the $\chi_{c0}\omega$, $J/\psi\eta$ and $X(3872)\gamma$ channels are fitted to the corresponding cross sections.

3. In the last step, the parameters obtained in the previous two steps are used as initial parameters for a global fit to all observables.

2.1 $e^+e^- \to D^0D^{*-}\pi^+$

The $D_1(2420)$ predominantly decay to the D-wave $D^*\pi$, which makes the $D_1\bar{D}$ molecular $Y(4230)$ predominantly decay to the $D^*\bar{D}\pi$ channel. The corresponding diagrams are shown in Fig. 2. The fitted lineshape, the corresponding invariant mass distributions of the sub two-body systems and the pion Jackson angular distribution are presented in Fig. 3. Diagram (a) is the D_1 tree-level contribution with its contribution illustrated by pink dot-dashed curves in Fig. 3. The diagram (b) is the contribution of $Y(4230)$ contact term with its contribution parameterized in respect with Watson theorem [37]. Its contribution is indicated by blue dashed curves. Diagram (c) is the D_1 triangle diagram with its contribution by the green long dashed curves. Its contribution is enhanced by a very close by triangle singularity [40]. Thus we expect diagrams (a) and (c) to

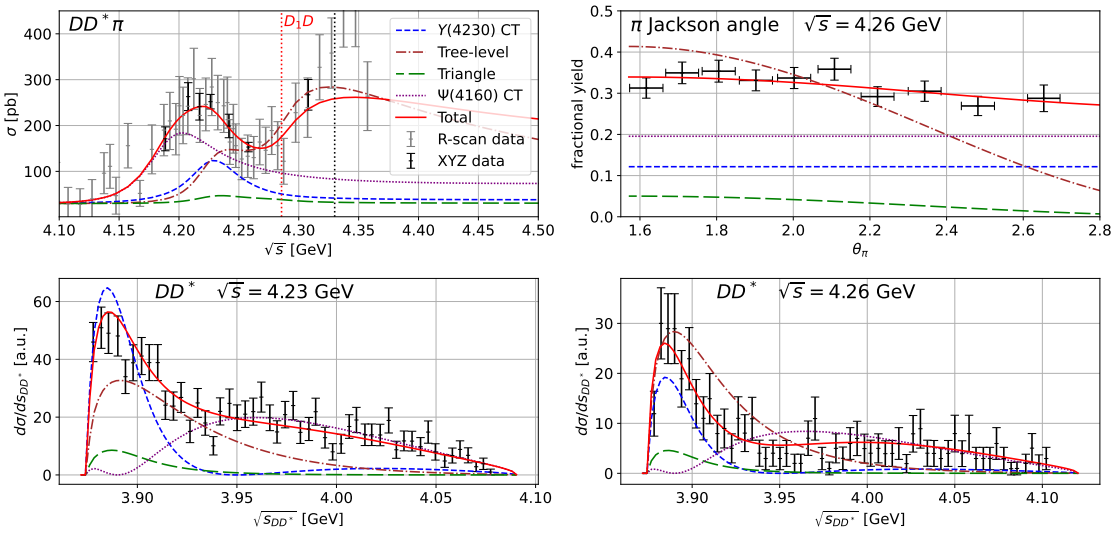

Figure 3: Fit results for the $D^0D^{*-}\pi$ cross section, the D^0D^{*-} invariant mass distribution and the pion Jackson angle. $D^0D^{*-}\pi^+$ R-scan and XYZ data are from Ref. [38], D^0D^{*-} invariant mass distribution is from Ref. [39].

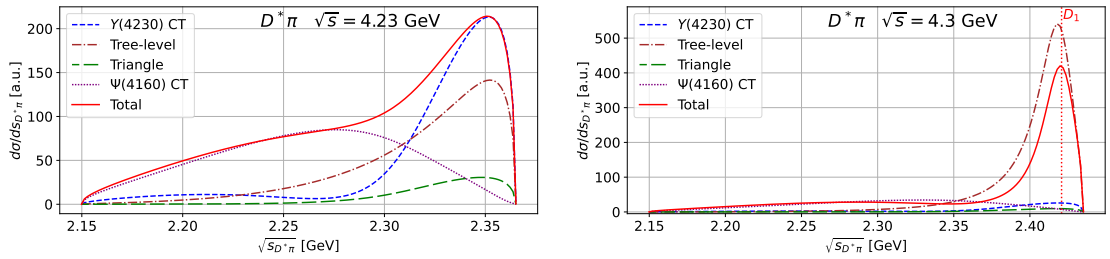

Figure 4: Predictions for the $D^*\pi$ invariant mass distributions at center-of-mass energies 4.23 GeV (left panel) and 4.3 GeV (right panel).

contribute significantly to the observables. Diagram (d) is $\psi(4160)$ contact contribution by the purple dotted curves.

We can see from the figure that both the tree-level and triangle diagrams have significant $D_1\bar{D}$ threshold effect. With the fitted parameters, we extract the pole position $(4227 \pm 4) - (25^{+4}_{-1})i$ MeV of the $Y(4230)$. The uncertainty is estimated by the uncertainties of the bare mass, the inelastic and the bare coupling to the $D_1\bar{D}$ channel of the $Y(4230)$ state in the $J/\psi\pi\pi$ channel. The extracted $Z_c(3900)$ pole is $3884 - 22i$ MeV with its mass higher than that of Ref. [41]. One can see that both the contributions of the Z_c and the D_1 give enhancements at the lower $D\bar{D}^*$ (Fig. 3) and higher $\bar{D}^*\pi$ (Fig. 4) invariant mass distributions. The total contribution of the D-wave and S-wave gives a flat pion angular distribution, which describes the data very well.

2.2 $e^+e^- \to J/\psi(\pi\pi/\bar{K}K)$

Figure 5 present the leading diagrams to the $e^+e^- \to J/\psi\pi\pi$ process. (a) and (b) are the box contributions which are illustrated by blue dashed curves in Fig. 6 (c) is the triangle diagram with its contribution illustrated by the green dotted curve. (e) is the $J/\psi\pi$ contact term (purple

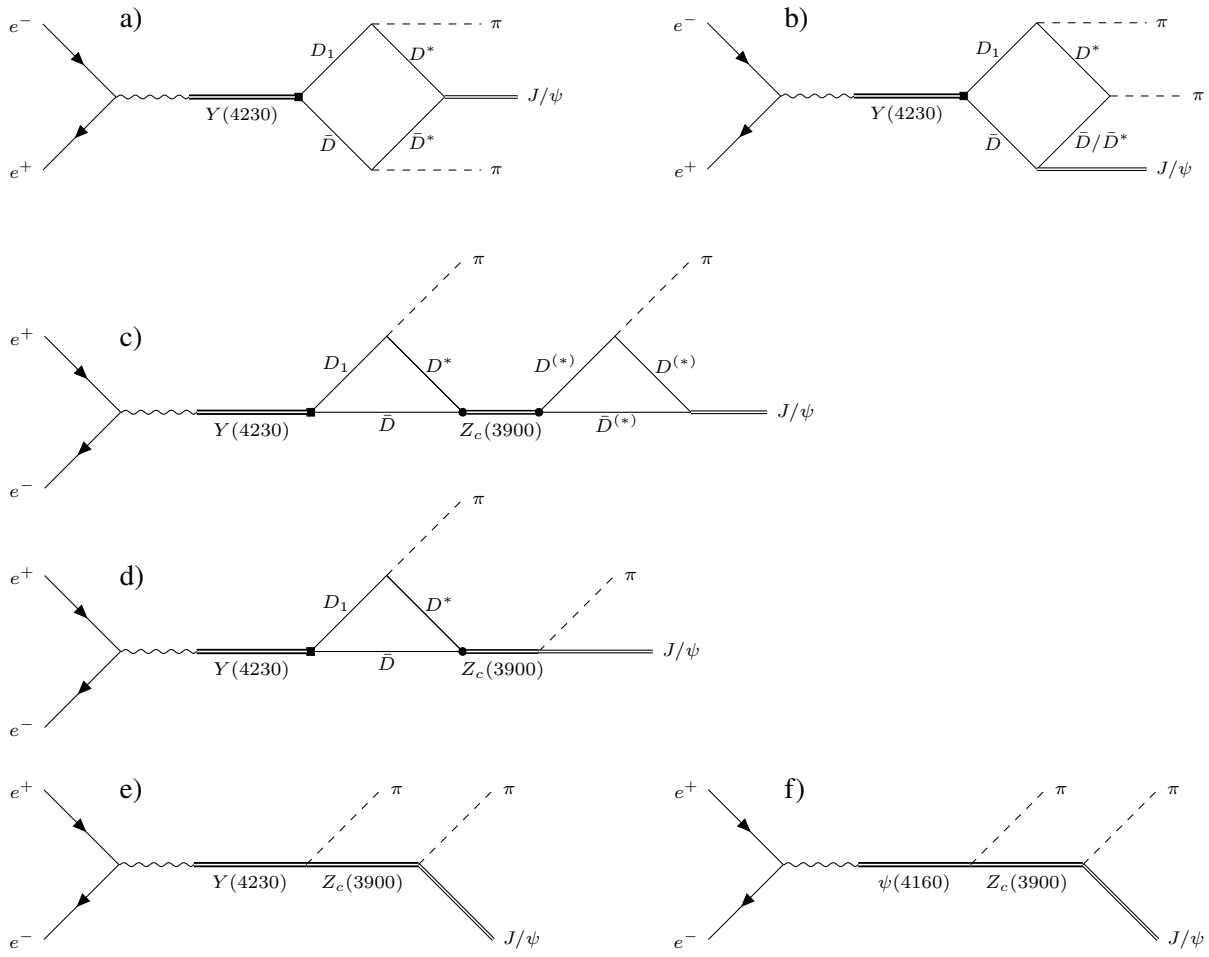

Figure 5: Diagram contributing to $e^+e^- \to J/\psi\pi\pi$. The thin lines in the box and triangle denote D^* or D mesons. a) and b) boxes, c) triangle, d) triangle counter term, e) $Y(4230)$ contact term, f) $\psi(4160)$ contact term, where for the last two the $J/\psi\pi$ final state interactions are included.

dot-dashed curve in Fig. 6). In diagram (e), we also include the $\pi\pi - K\bar{K}$ final state interaction [42–45] which also naturally gives the $J/\psi K\bar{K}$ lineshape (Fig. 6). The large asymmetric lineshape emerge at the $D_1\bar{D}$ threshold for both box and triangle diagrams. The leading effect for the $J/\psi K\bar{K}$ channel is driven by the $\pi\pi - K\bar{K}$ final state interaction. The $\pi\pi - \bar{K}K$ coupled channel treatment provides us at the same time access to $J/\psi\bar{K}K$ final state. The strangeness source is driven by the strange box diagram, which does not introduce any additional parameters due to the SU(3) flavor symmetry. When the center-of-mass energy goes beyond the $D_s^{*+}\bar{D}K^-$ threshold, the strange source is important.

2.3 $e^+e^- \to h_c\pi\pi$

For the $h_c\pi\pi$ channel, we only include the box diagrams analogous to those for the $J/\psi\pi\pi$ channel shown in Fig. 5. However, in contrast to the $J/\psi\pi\pi$ channel, we exclude diagrams containing a $Z_c(3900)$. This is based on the observation that $Z_c(3900)$ does not show a significant

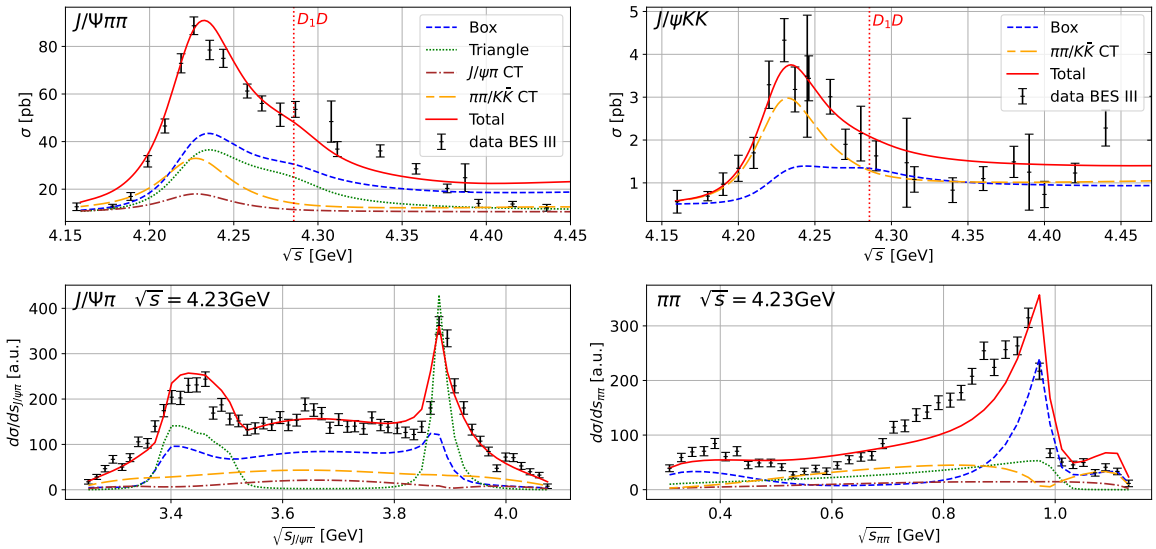

Figure 6: Fit results for the $J/\psi\pi^+\pi^-$ cross section [2] and the $J/\psi\pi^\pm$ and $\pi^+\pi^-$ [46] invariant mass distributions. The data for the $J/\psi K\bar{K}$ channel are taken from Ref. [13].

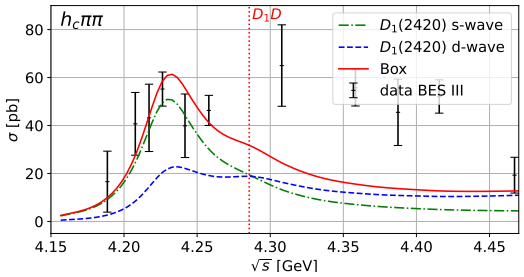

Figure 7: Prediction for the $h_c\pi^+\pi^-$ cross section. The data are taken from Ref. [7].

contribution to the $h_c\pi$ invariant mass distribution. Additionally, we point out that the $Z_c(4020)$ is not included in this work, since this would require a complete treatment of the $\{D_1\bar{D}^{(*)}, D_2\bar{D}^{(*)}\}$ coupled channels for the vector charmonium-like states and of the $\{D\bar{D}^*, D^*\bar{D}^*\}$ for the subsystems. Another consideration is that we do not expect the effect of $Z_c(4020)$ on a significant structure in the total cross section of $h_c\pi\pi$, which has been demonstrated for the $Z_c(3900)$ in the $J/\psi\pi$ channel. One can see that the total cross section of the $h_c\pi\pi$ channel is of the same order as that of the $J/\psi\pi\pi$ channel(Fig. 7), which indicates a large Heavy Quark Spin Symmetry (HQSS) violation in the molecular picture.

2.4 $e^+e^- \to X(3872)\gamma, J/\psi\eta, \chi_{c0}\omega$

Under the assumption that the $Y(4230)$ is a $D_1\bar{D}$ hadronic molecule, its decays to the isospin triplet $D^*\bar{D}$ hadronic molecule $Z_c(3900)$ and the isospin singlet $D^*\bar{D}$ hadronic molecule $X(3872)$ are analogous [47]. Thus, we first consider the $X(3872)\gamma$ two-body final state. For this channel, both the triangle diagram and the contact contributions of the $Y(4230)$ and the $\psi(4160)$ are considered (Fig. 8). The considered diagrams for the $J/\psi\eta$ and $\chi_{c0}\omega$ processes are analogous (Ref. [37]).

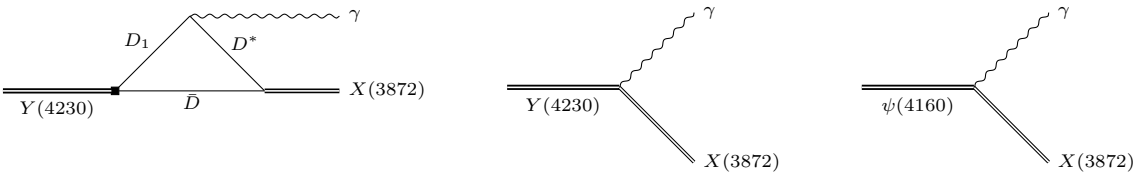

Figure 8: Diagrams for the $Y(4230) \to X(3872)\gamma$ process.

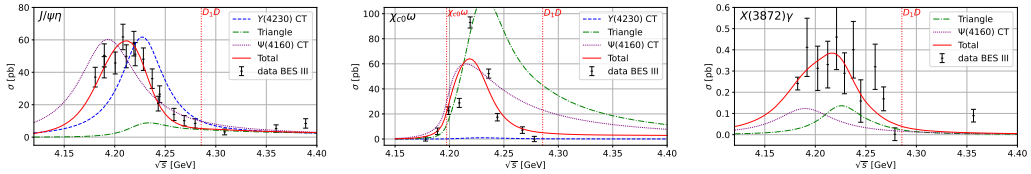

Figure 9: Fit results for the $e^+e^- \to J/\psi\eta$, $e^+e^- \to \chi_{c0}\omega$ and $e^+e^- \to X(3872)\gamma$ cross section. The data sets are taken from Ref. [8], Ref. [9], and Ref. [11], respectively.

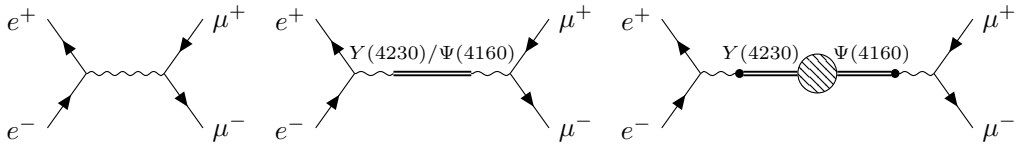

Figure 10: Diagrams contributing to $e^+e^- \to \mu^+\mu^-$. The hatched circle in the rightmost diagram is the mixing of the two vector states driven by their common decays to the channels $DD^*\pi, J/\psi\pi\pi, \chi_{c0}\omega, J/\psi\eta$ and $X(3872)\gamma$ considered in this analysis.

The fitted results for these three two-body channels can be found in Fig. 9. One can see that the contributions of the triangle diagram and the $\psi(4160)$ are constructive and destructive in $X(3872)\gamma$ and $\chi_{c0}\omega$ channels, respectively. In the $\chi_{c0}\omega$ channel, the convolution of the ω width is taken into account. The statistic of the experimental data in the two-body channel are still not sufficient.

2.5 $e^+e^- \to \mu^+\mu^-$

The reason why we are interested in the $e^+e^- \to \mu^+\mu^-$ process is that it may isolate production from decay, since the total cross section is by far dominated by the real valued tree-level diagram (first diagram in Fig. 10) and the hadronic cross sections only contribute significantly through their interference with the mentioned dominating one. The mixing of the two vector resonances is depicted here as the hatched blob. The imaginary part of this mixing amplitude is given by the respective interference terms that contribute also to the various exclusive hadronic channels discussed above. Therefore, the simultaneous study of the hadronic channels and the $e^+e^- \to \mu^+\mu^-$ channel provides a sanity check for the size of the induced mixing of the vector states, which turn out to be significant.

The results for the $e^+e^- \to \mu^+\mu^-$ process are shown by the left panel of Fig. 11. The cross section is completely dominated by the real tree level amplitude. Accordingly, following Eq. (1)

$$\sigma_{e^+e^-\to\mu^+\mu^-} = \sigma^{\text{tree}}_{e^+e^-\to\mu^+\mu^-} \times |1+\mathcal{A}_R+\mathcal{A}_{\text{mix}}|^2$$

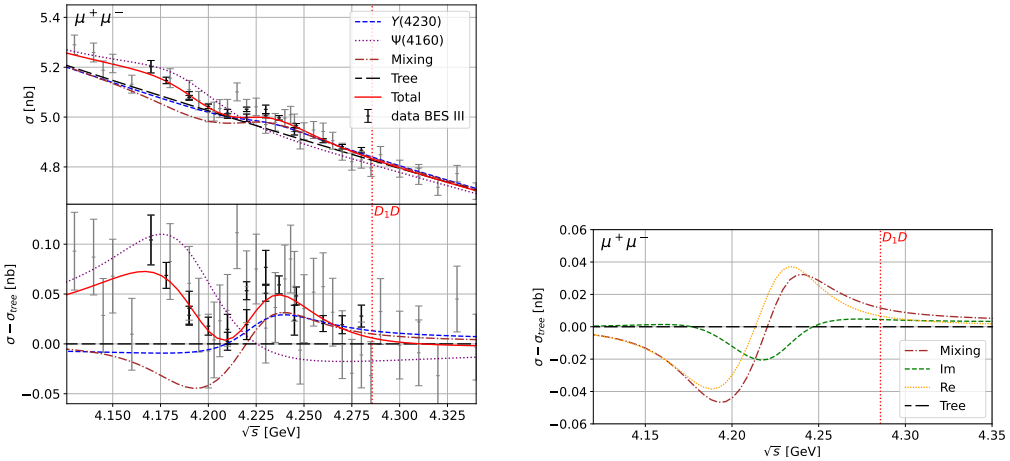

Figure 11: Left panel: Fit results for the $\mu^+\mu^-$ cross section. The measured born cross section (upper panel) and that with the cross section from the tree level amplitude subtracted (lower panel) in comparison with the experimental data [12]. Right panel: Contributions of the real (orange dotted line) and imaginary (green dashed line) parts from the mixing of $Y(4230)$ and $\Psi(4160)$ to the cross section.

the signal of interest to us reads to very good approximation

$$\sigma_{e^+e^-\to\mu^+\mu^-} - \sigma^{\text{tree}}_{e^+e^-\to\mu^+\mu^-} \approx 2\sigma^{\text{tree}}_{e^+e^-\to\mu^+\mu^-}\text{Re}(\mathcal{A}_R + \mathcal{A}_{\text{mix}}) \ .$$

This contribution is presented in the left-lower panel of Fig. 11. One can see that the real and the imaginary part of the mixing amplitude are of comparable strength (right panel of Fig. 11). To better describe the data, especially the $e^+e^- \to \mu^+\mu^-$ data, a complex phase between charmonium and virtual photon is included. This complex phase non-trivially mixes the real and imaginary parts of the mixing amplitude, allowing both contributions to interfere with the tree level amplitude. We see that the contribution of the $\psi(4160)$ is more dominant than that of the $Y(4230)$ in the energy below 4.2 GeV. The peak at 4.23 GeV emerges from the interference of the two resonances and the $Y(4230)$ itself. The main predominant contribution to the imaginary part is the mixing between the $\psi(4160)$ and the $Y(4230)$.

3. Summary and outlook

In this work, we simultaneously analyze the lineshapes of the eight channels in electron-positron annihilation in a phenomenological way. The large asymmetric lineshapes stems from the $D_1\bar{D}$ threshold. A combined fit of all the channels indicates a single vector charmonium-like state $Y(4230)$ emerging in the energy region $[4.2, 4.35]$ GeV with its pole position $M^{\text{pole}}_{Y(4230)} = (4227 \pm 4) - i(25^{+4}_{-1})$ MeV. A pole $M^{\text{pole}}_{Z_c(3900)} = 3884 - 22i$ MeV in the subsystems also exists, which corresponds to the $Z_c(3900)$. Besides the vector charmonium-like state $Y(4230)$, the analysis also requires the presence of the conventional charmonium $\psi(4160)$, especially around the energy 4.2 GeV in the $e^+e^- \to \mu^+\mu^-$ cross section. Our analysis is phenomenological and partly considers the $\pi\pi - K\bar{K}$ final state interaction. To better control the uncertainty of this analysis, a rigorous framework in effective field theory should be developed.

We thank Ryan Mitchell for the idea to allow for the interference with lower lying vector states to achieve a simultaneous description of the various channels. This work is supported in part by the Deutsche Forschungsgemeinschaft (DFG) through the funds provided to the Sino-German Collaborative Research Center TRR110 "Symmetries and the Emergence of Structure in QCD" (NSFC Grant No. 12070131001, DFG Project-ID 196253076), by the NSFC under Grants No. 11835015, No. 12047503, No. 11961141012, No. 12035007, and No. 12375073 and by the Chinese Academy of Sciences under Grants No. QYZDB-SSW-SYS013, No. XDB34030000, No. XDPB15 and No. 2020VMA0024. The work of Q.W. is also supported by Guangdong Major Project of Basic and Applied Basic Research under Grant No. 2020B0301030008, by the Science and Technology Program of Guangzhou under Grant No. 2019050001, and by Guangdong Provincial funding under Grant No. 2019QN01X172.

References

[1] M. Ablikim *et al.* [BESIII], *Precise measurement of the* $e^+e^- \to \pi^+\pi^- J/\psi$ *cross section at center-of-mass energies from 3.77 to 4.60 GeV*, Phys. Rev. Lett. **118**, no.9, 092001 (2017), (doi:10.1103/PhysRevLett.118.092001 [arXiv:1611.01317 [hep-ex]]).

[2] M. Ablikim *et al.* [BESIII], *Study of the resonance structures in the process* $e^+e^+ \to \pi^+\pi^- J/\psi$, Phys. Rev. D **106**, no.7, 072001 (2022), (doi:10.1103/PhysRevD.106.072001 [arXiv:2206.08554 [hep-ex]]).

[3] M. Ablikim *et al.* [BESIII], *Study of the process* $e^+e^- \to \pi^0\pi^0 J/\psi$ *and neutral charmonium-like state* $Z_c(3900)^0$, Phys. Rev. D **102**, no.1, 012009 (2020), (doi:10.1103/PhysRevD.102.012009 [arXiv:2004.13788 [hep-ex]]).

[4] J. P. Lees *et al.* [BaBar], *Study of the reaction* $e^+e^- \to \psi(2S)\pi^-\pi^-$ *via initial-state radiation at BaBar*, Phys. Rev. D **89**, no.11, 111103 (2014), (doi:10.1103/PhysRevD.89.111103 [arXiv:1211.6271 [hep-ex]]).

[5] X. L. Wang *et al.* [Belle], *Measurement of* $e^+e^- \to \pi^+\pi^-\psi(2S)$ *via Initial State Radiation at Belle*, Phys. Rev. D **91**, 112007 (2015), (doi:10.1103/PhysRevD.91.112007 [arXiv:1410.7641 [hep-ex]]).

[6] M. Ablikim *et al.* [BESIII], *Cross section measurement of* $e^+e^- \to \pi^+\pi^-\psi(3686)$ *from* $\sqrt{s}$ = 4.0076 *to 4.6984 GeV*, Phys. Rev. D **104**, no.5, 052012 (2021), (doi:10.1103/PhysRevD.104.052012 [arXiv:2107.09210 [hep-ex]]).

[7] M. Ablikim *et al.* [BESIII], *Evidence of Two Resonant Structures in* $e^+e^- \to \pi^+\pi^- h_c$, Phys. Rev. Lett. **118**, no.9, 092002 (2017), (doi:10.1103/PhysRevLett.118.092002 [arXiv:1610.07044 [hep-ex]]).

[8] M. Ablikim *et al.* [BESIII], *Observation of the* $Y(4220)$ *and* $Y(4360)$ *in the process* $e^+e^- \to \eta J/\psi$, Phys. Rev. D **102**, no.3, 031101 (2020), (doi:10.1103/PhysRevD.102.031101 [arXiv:2003.03705 [hep-ex]]).

[9] M. Ablikim *et al.* [BESIII], *Cross section measurements of $e^+e^- \to \omega\chi_{c0}$ form $\sqrt{s}$ = 4.178 to 4.278 GeV*, Phys. Rev. D **99**, no.9, 091103 (2019), (doi:10.1103/PhysRevD.99.091103 [arXiv:1903.02359 [hep-ex]]).

[10] M. Ablikim *et al.* [BESIII], *Evidence of a resonant structure in the $e^+e^- \to \pi^+D^0D^{*-}$ cross section between 4.05 and 4.60 GeV*, Phys. Rev. Lett. **122**, no.10, 102002 (2019), (doi:10.1103/PhysRevLett.122.102002 [arXiv:1808.02847 [hep-ex]]).

[11] M. Ablikim *et al.* [BESIII], *Study of $e^+e^- \to \gamma\omega J/\psi$ and Observation of $X(3872) \to \omega J/\psi$*, Phys. Rev. Lett. **122**, no.23, 232002 (2019), (doi:10.1103/PhysRevLett.122.232002 [arXiv:1903.04695 [hep-ex]]).

[12] [BESIII], *Measurement of cross sections for $e^+e^- \to \mu^+\mu^-$ at center-of-mass energies from 3.80 to 4.60 GeV*, Phys. Rev. D **102**, 112009 (2020), (doi:10.1103/PhysRevD.102.112009 [arXiv:2007.12872 [hep-ex]]).

[13] M. Ablikim *et al.* [(BESIII), and BESIII], *Observation of the Y(4230) and a new structure in $e^+e^- \to K^+K^-J/\psi$*, Chin. Phys. C **46**, no.11, 111002 (2022), (doi:10.1088/1674-1137/ac945c [arXiv:2204.07800 [hep-ex]]).

[14] S. Dubynskiy and M. B. Voloshin, *Hadro-Charmonium*, Phys. Lett. B **666**, 344-346 (2008), (doi:10.1016/j.physletb.2008.07.086 [arXiv:0803.2224 [hep-ph]]).

[15] X. Li and M. B. Voloshin, *Y(4260) and Y(4360) as mixed hadrocharmonium*, Mod. Phys. Lett. A **29**, no.12, 1450060 (2014), (doi:10.1142/S0217732314500606 [arXiv:1309.1681 [hep-ph]]).

[16] M. Cleven, F. K. Guo, C. Hanhart, Q. Wang and Q. Zhao, *Employing spin symmetry to disentangle different models for the XYZ states*, Phys. Rev. D **92**, no.1, 014005 (2015), (doi:10.1103/PhysRevD.92.014005 [arXiv:1505.01771 [hep-ph]]).

[17] F. E. Close and P. R. Page, *Gluonic charmonium resonances at BaBar and BELLE?*, Phys. Lett. B **628**, 215-222 (2005), (doi:10.1016/j.physletb.2005.09.016 [arXiv:hep-ph/0507199 [hep-ph]]).

[18] E. Kou and O. Pene, *Suppressed decay into open charm for the Y(4260) being an hybrid*, Phys. Lett. B **631**, 164-169 (2005), (doi:10.1016/j.physletb.2005.09.013 [arXiv:hep-ph/0507119 [hep-ph]]).

[19] Y. S. Kalashnikova and A. V. Nefediev, *Spectra and decays of hybrid charmonia*, Phys. Rev. D **77**, 054025 (2008), (doi:10.1103/PhysRevD.77.054025 [arXiv:0801.2036 [hep-ph]]).

[20] M. Berwein, N. Brambilla, J. Tarrús Castellà and A. Vairo, *Quarkonium Hybrids with Nonrelativistic Effective Field Theories*, Phys. Rev. D **92**, no.11, 114019 (2015), (doi:10.1103/PhysRevD.92.114019 [arXiv:1510.04299 [hep-ph]]).

[21] N. Brambilla, W. K. Lai, A. Mohapatra and A. Vairo, *Heavy hybrid decays to quarkonia*, Phys. Rev. D **107**, no.5, 054034 (2023), (doi:10.1103/PhysRevD.107.054034 [arXiv:2212.09187 [hep-ph]]).

[22] A. Ali, L. Maiani, A. V. Borisov, I. Ahmed, M. Jamil Aslam, A. Y. Parkhomenko, A. D. Polosa and A. Rehman, *A new look at the Y tetraquarks and Ω_c baryons in the diquark model*, Eur. Phys. J. C **78**, no.1, 29 (2018), (doi:10.1140/epjc/s10052-017-5501-6 [arXiv:1708.04650 [hep-ph]]).

[23] T. Bhavsar, M. Shah, S. Patel and P. C. Vinodkumar, *Masses of tetraquark states in the hidden charm sector above $D - D^*$ threshold*, Nucl. Phys. A **1000**, 121856 (2020), (doi:10.1016/j.nuclphysa.2020.121856 [arXiv:2002.06363 [hep-ph]]).

[24] M. Shifman, *QCD chemistry: Remarks on diquarks*, Nucl. Part. Phys. Proc. **347**, 86-89 (2024) (doi:10.1016/j.nuclphysbps.2024.10.007 [arXiv:2412.05440 [hep-ph]]).

[25] R. F. Lebed, *Spectroscopy of Exotic Hadrons Formed from Dynamical Diquarks*, Phys. Rev. D **96**, no.11, 116003 (2017), (doi:10.1103/PhysRevD.96.116003 [arXiv:1709.06097 [hep-ph]]).

[26] G. J. Ding, *Are $Y(4260)$ and $Z_2^+(4250)$ are D_1D or D_0D^* Hadronic Molecules?*, Phys. Rev. D **79**, 014001 (2009), (doi:10.1103/PhysRevD.79.014001 [arXiv:0809.4818 [hep-ph]]).

[27] Q. Wang, C. Hanhart and Q. Zhao, *Decoding the riddle of $Y(4260)$ and $Z_c(3900)$*, Phys. Rev. Lett. **111**, no.13, 132003 (2013), (doi:10.1103/PhysRevLett.111.132003 [arXiv:1303.6355 [hep-ph]]).

[28] S. Coito and F. Giacosa, *On the Origin of the $Y(4260)$*, Acta Phys. Polon. B **51**, no.8, 1713-1737 (2020), (doi:10.5506/APhysPolB.51.1713 [arXiv:1902.09268 [hep-ph]]).

[29] D. Y. Chen, X. Liu, X. Q. Li and H. W. Ke, *Unified Fano-like interference picture for charmoniumlike states Y(4008), Y(4260) and Y(4360)*, Phys. Rev. D **93**, 014011 (2016), (doi:10.1103/PhysRevD.93.014011 [arXiv:1512.04157 [hep-ph]]).

[30] M. Cleven, Q. Wang, F. K. Guo, C. Hanhart, U.-G. Meißner and Q. Zhao, *$Y(4260)$ as the first S-wave open charm vector molecular state?*, Phys. Rev. D **90**, no.7, 074039 (2014), (doi:10.1103/PhysRevD.90.074039 [arXiv:1310.2190 [hep-ph]]).

[31] W. Qin, S. R. Xue and Q. Zhao, *Production of $Y(4260)$ as a hadronic molecule state of $\bar{D}D_1 + c.c.$ in e^+e^- annihilations*, Phys. Rev. D **94**, no.5, 054035 (2016), (doi:10.1103/PhysRevD.94.054035 [arXiv:1605.02407 [hep-ph]]).

[32] S. Weinberg, *Evidence That the Deuteron Is Not an Elementary Particle*, Phys. Rev. **137**, B672-B678 (1965), (doi:10.1103/PhysRev.137.B672).

[33] L.D. Landau, Soviet Zh. Eksp. Teor. Fiz. **39**, 1856(1960)

[34] F. K. Guo, C. Hanhart, U.-G. Meißner, Q. Wang, Q. Zhao and B. S. Zou, *Hadronic molecules*, Rev. Mod. Phys. **90**, no.1, 015004 (2018) [erratum: Rev. Mod. Phys. **94**, no.2, 029901 (2022)], (doi:10.1103/RevModPhys.90.015004 [arXiv:1705.00141 [hep-ph]]).

[35] F. K. Guo, C. Hanhart and U.-G. Meißner, *On the extraction of the light quark mass ratio from the decays $\psi' \to J/\psi\pi^0(\eta)$*, Phys. Rev. Lett. **103**, 082003 (2009) [erratum: Phys. Rev. Lett. **104**, 109901 (2010)], (doi:10.1103/PhysRevLett.103.082003 [arXiv:0907.0521 [hep-ph]]).

[36] F. K. Guo, C. Hanhart, G. Li, U.-G. Meißner and Q. Zhao, *Effect of charmed meson loops on charmonium transitions*, Phys. Rev. D **83**, 034013 (2011), (doi:10.1103/PhysRevD.83.034013 [arXiv:1008.3632 [hep-ph]]).

[37] L. von Detten, V. Baru, C. Hanhart, Q. Wang, D. Winney and Q. Zhao, *How many vector charmoniumlike states lie in the mass range 4.2–4.35 GeV?*, Phys. Rev. D **109**, no.11, 116002 (2024), (doi:10.1103/PhysRevD.109.116002 [arXiv:2402.03057 [hep-ph]]).

[38] M. Ablikim *et al.* [BESIII], *Observation of Three Charmoniumlike States with* $J^{PC} = 1^{--}$ *in* $e^+e^- \to D^{*0}D^{*-}\pi^+$, Phys. Rev. Lett. **130**, no.12, 121901 (2023), (doi:10.1103/PhysRevLett.130.121901 [arXiv:2301.07321 [hep-ex]]).

[39] M. Ablikim *et al.* [BESIII], *Confirmation of a charged charmoniumlike state* $Z_c(3885)^{\mp}$ *in* $e^+e^- \to \pi^{\pm}(D\bar{D}^*)^{\mp}$ *with double D tag*, Phys. Rev. D **92**, no.9, 092006 (2015), (doi:10.1103/PhysRevD.92.092006 [arXiv:1509.01398 [hep-ex]]).

[40] Q. Wang, C. Hanhart and Q. Zhao, *Systematic study of the singularity mechanism in heavy quarkonium decays*, Phys. Lett. B **725**, no.1-3, 106-110 (2013), (doi:10.1016/j.physletb.2013.06.049 [arXiv:1305.1997 [hep-ph]]).

[41] Y. H. Chen, M. L. Du and F. K. Guo, *Precise determination of the pole position of the exotic* $Z_c(3900)$, Sci. China Phys. Mech. Astron. **67**, no.9, 291011 (2024), (doi:10.1007/s11433-023-2408-1 [arXiv:2310.15965 [hep-ph]]).

[42] I. Danilkin, D. A. S. Molnar and M. Vanderhaeghen, *Simultaneous description of the* $e^+e^- \to J/\psi\,\pi\pi\,(K\bar{K})$ *processes*, Phys. Rev. D **102**, no.1, 016019 (2020), (doi:10.1103/PhysRevD.102.016019 [arXiv:2004.13499 [hep-ph]]).

[43] Y. H. Chen, J. T. Daub, F. K. Guo, B. Kubis, U.-G. Meißner and B. S. Zou, *Effect of* Z_b *states on* $\Upsilon(3S) \to \Upsilon(1S)\pi\pi$ *decays*, Phys. Rev. D **93**, no.3, 034030 (2016), (doi:10.1103/PhysRevD.93.034030 [arXiv:1512.03583 [hep-ph]]).

[44] Y. H. Chen, M. Cleven, J. T. Daub, F. K. Guo, C. Hanhart, B. Kubis, U.-G. Meißner and B. S. Zou, *Effects of* Z_b *states and bottom meson loops on* $\Upsilon(4S) \to \Upsilon(1S, 2S)\pi^+\pi^-$ *transitions*, Phys. Rev. D **95**, no.3, 034022 (2017), (doi:10.1103/PhysRevD.95.034022 [arXiv:1611.00913 [hep-ph]]).

[45] V. Baru, E. Epelbaum, A. A. Filin, C. Hanhart, R. V. Mizuk, A. V. Nefediev and S. Ropertz, *Insights into* $Z_b(10610)$ *and* $Z_b(10650)$ *from dipion transitions from* $\Upsilon(10860)$, Phys. Rev. D **103**, no.3, 034016 (2021), (doi:10.1103/PhysRevD.103.034016 [arXiv:2012.05034 [hep-ph]]).

[46] M. Ablikim *et al.* [BESIII], *Determination of the Spin and Parity of the* $Z_c(3900)$, Phys. Rev. Lett. **119**, no.7, 072001 (2017), (doi:10.1103/PhysRevLett.119.072001 [arXiv:1706.04100 [hep-ex]]).

[47] F. K. Guo, C. Hanhart, U.-G. Meißner, Q. Wang and Q. Zhao, *Production of the X(3872) in charmonia radiative decays*, Phys. Lett. B **725**, 127-133 (2013), (doi:10.1016/j.physletb.2013.06.053 [arXiv:1306.3096 [hep-ph]]).